Surface resistivity of semi-infinite crystals

H. Ishida
College of Humanities and Sciences, Nihon University, Sakura-josui, Tokyo 156, Japan
(Received 29 July 1997)

The surface resistivity of low-index surfaces of Al is evaluated by a first-principles density-functional calculation. Contrary to the naive expectation that the close-packed (111) surface of fcc metals would scatter conduction electrons in the metal nearly specularly, the calculated resistivity of Al(111) is found to be much larger than that of the more loosely packed Al(001) surface. The large difference between the two surfaces is not related to the strength of the surface scattering potential. Instead, it simply arises from the fact that the fcc crystal has no reflection symmetry about the (111) crystal plane, which means that there is in general no Bloch wave corresponding to specular reflection when a conduction electron in the metal is incident on the (111) surface. [S0163-1829(98)00908-4]

I. INTRODUCTION

When Bloch electrons incident from the interior of metals are elastically scattered at the surface, their velocity in the plane can be changed. This scattering process contributes to the resistivity of the metal, as does the impurity scattering. Experimentally, it is known that the resistivity of a thin metallic film with thickness $l_f = 10^2 - 10^3$ Å is very sensitive to surface conditions such as adsorbates and steps at low temperatures.[1] The surface resistivity is related to other dynamical quantities at the surface such as the electronic friction force exerted on adatoms[2] and the nonlocal corrections to the local Fresnel optics.[3] In the present work, we evaluate the resistivity of clean surfaces of semi-infinite metals. It might appear that ideal crystal surfaces without defects should have no resistivity, since the surface retains the symmetry of the bulk crystal in the surface plane. Looking more closely, one sees that there are two scattering processes contributing to finite resistivity.

Let us consider a semi-infinite crystal surface made of atomic lattice planes piled up in the z direction. The z axis is taken as a surface normal pointing toward the vacuum. To specify a Bloch state in the bulk crystal, we use index $\xi = (\mathbf{K}, n)$, where $\mathbf{K} = (\mathbf{k}, k_z)$ is the three-dimensional (3D) wave vector in the 3D Brillouin zone, and n is the band index. The wave function and energy of state ξ are denoted by ϕ_ξ and $\epsilon(\xi)$. The α component of its velocity is given by $v_\alpha(\xi) = \hbar^{-1} \partial \epsilon(\xi) / \partial k_\alpha$. In the case of defect-free ideal crystal surfaces, the electron crystal momentum in the plane, $\mathbf{k}$, is conserved when conduction electrons in the metal are scattered at the surface. However, their velocity in the plane can be changed via the two mechanisms. The first is an analogy to low-energy electron-diffraction (LEED) experiments where electrons incident from the vacuum are scattered at the surface, and part of them are scattered in off-specular directions via the Umklapp process. In the present case, electrons are incident from the interior of the metal, but the same process can take place if there is more than one reflected wave $\phi_{\xi'}$ with $v_z(\xi') < 0$ for a given $\mathbf{k}$ in the surface Brillouin zone (SBZ). This is generally the case for multivalence metals with several occupied energy bands, or if the SBZ is reduced due to the formation of surface superstructures. The second mechanism stems from the symmetry of the crystal plane corresponding to the surface. If the bulk metal has a reflection symmetry about the xy plane, for a given incident Bloch wave ϕ_ξ with $\xi = (\mathbf{k}, k_z, n)$ and $v_z(\xi) > 0$, there always exists a specularly reflected wave $\phi_{\xi'}$ with $\xi' = (\mathbf{k}, -k_z, n)$. On the other hand, if this symmetry is absent, the two $\mathbf{K}$ points, $(\mathbf{k}, k_z)$ and $(\mathbf{k}, -k_z)$, are not symmetrically equivalent, which indicates that there is in general no specularly reflected wave $\phi_{\xi'}$ corresponding to the incident wave ϕ_ξ. Thus, essentially, all the conduction electrons impinging on the surface are reflected off-specularly and contribute to the surface resistivity.

As an example, let us consider alkali metals (bcc) with a half-filled valence s band. For these metals, the LEED mechanism is excluded. Thus the resistivity of the (110) and (001) surfaces of alkali metals vanishes identically, whereas their (111) surfaces should have nonvanishing resistivity due to the second mechanism if it is very small. Similarly, the close-packed (111) surface of a fcc crystal may have larger resistivity than its more loosely packed (001) surface, which is counterintuitive. In order to explore the significance of these mechanisms, we perform a density-functional calculation for semi-infinite Al surfaces. It will be shown that the resistivity of the Al(111) surface is actually by ~ 6 times larger than that of the Al(001) surface.

The plan of the present paper is as follows. In Sec. II, we give a microscopic expression of the surface resistivity for semi-infinite crystals, and describe a numerical method for evaluating it for the case of clean metal surfaces. In Sec. III we present results and a discussion of the numerical calculation for the Al(111) and Al(001) surfaces. Finally, a short summary is given in Sec. IV.

II. THEORY

Recently we derived a microscopic expression of the dc surface resitivity for semi-infinite metals.[4] In that work, the interior of the metal was treated as jellium. A more generalized expression, which is applicable to arbitrary semi-infinite crystal surfaces with and without surface defects, is

$$[Sl_f]\ \rho_s^{\alpha\beta}=\sum_{\alpha',\beta'}\frac{m^*_{\alpha\alpha'}m^*_{\beta'\beta}}{2\pi\hbar n_e^2e^2}\sum_{\xi,\xi'}[\Delta v_{\alpha'}\Delta v_{\beta'}]p(\epsilon_F,\xi,\xi'), \tag{1}$$

where S, the area of the surface, and l_f, the thickness of the film, are macroscopic quantities, n_e is the number density of conduction electrons in the metal, ϵ_F is the Fermi energy, $\Delta v_\alpha=v_\alpha(\xi')-v_\alpha(\xi)$, and $p(\epsilon,\xi,\xi')$ denotes the probability that an incident Bloch electron ϕ_ξ is elastically scattered at the surface and reflected as a scattered wave $\phi_{\xi'}$. The current conservation implies $\Sigma_{\xi'}p(\epsilon,\xi,\xi')=1$. The summation over ξ (ξ') in Eq. (1) signifies $\int S\ d\mathbf{k}/(2\pi)^2\Sigma_{k_z,n}$, that is, the SBZ integration and discrete summation at each $\mathbf{k}$ point in the SBZ over the pairs of (k_z,n) satisfying the conditions $\epsilon(\xi)=\epsilon_F$ and $v_z(\xi)>0$ [$\epsilon(\xi')=\epsilon_F$ and $v_z(\xi')<0$]. The surface resistivity induces energy dissipation in the system per unit time, $P=[Sl_f]\Sigma_{\alpha,\beta}\rho_s^{\alpha\beta}J^*_\alpha J_\beta$, where J_α is the α (x or y) component of the macroscopic current density in the interior of the metal. Under the application of a uniform ac electric field parallel to the surface, $(E_x,E_y)\exp(-i\omega t)$, J_α is given to the lowest order of ω as $J_\alpha=(in_e e^2/\omega)\Sigma_\beta(1/m^*)_{\alpha\beta}E_\beta$, where $(1/m^*)_{\alpha\beta}$ stands for the average of $\hbar^{-2}\partial^2\epsilon(\xi)/\partial k_\alpha\partial k_\beta$ over all the occupied states. $m^*_{\alpha\beta}$ appearing in Eq. (1) is defined as the inverse of this 2×2 matrix. For a 3D crystal without the surface, P vanishes if $\hbar\omega$ is smaller than the minimum interband excitation energy, $\mathrm{Min}|\epsilon(\xi')-\epsilon(\xi)|$, where $\xi=(\mathbf{K},n)$ and $\xi'=(\mathbf{K},n')$ are the occupied and unoccupied Bloch states. For clean metal surfaces, $\mathbf{k}$ is conserved. However, P may remain finite even in the limit of $\omega\to0$ because of the absence of k_z conservation. This is why clean metallic surfaces can have finite dc resitivity. For very thin slabs, k_z is replaced by a discrete quantum number n_z. The resistivity in this case vanishes again if $\hbar\omega$ is smaller than the minimum interband excitation energy with respect to n_z.

For the semi-infinite surface geometry, the asymptotic form of one-electron wave functions in the interior of the metal is a sum of the incident and reflected Bloch waves,

$$\psi_\xi(\mathbf{r})=\frac{1}{\sqrt{S}}\left\{\frac{1}{v_z(\xi)}\ \phi_\xi(\mathbf{r})+\sum_{\xi'}\ r(\xi,\xi')\ \ \phi_{\xi'}(\mathbf{r})\right\}, \tag{2}$$

where $\mathbf{r}=(\mathbf{x},z)$, $v_z(\xi)>0$, $v_z(\xi')<0$, and $\epsilon(\xi)=\epsilon(\xi')=\epsilon$, and we omitted for simplicity the evanescent waves in the second term. As for the scattering amplitude, one can prove the reciprocity relation $r(\xi,\xi')=r(\xi'^*,\xi^*)$ where the symbol ξ^* indicates $(\phi_\xi)^*$. We normalize the bulk Bloch state ϕ_ξ in a unit volume. Then the scattering probability is given by

$$p(\epsilon,\xi,\xi')=-v_z(\xi)\ \ v_z(\xi')|r(\xi,\xi')|^2. \tag{3}$$

Equations (1) and (3) indicate that the surface resistivity can be estimated from the asymptotic form of one-electron wave functions at the Fermi energy alone. In the following, we describe a numerical method for determining ψ_ξ for semi-infinite clean surfaces. Those who are not interested in calculational details can skip over the rest of this section.

Widely used repeated-slab techniques for the surface electronic-structure calculation provide little information on the scattering amplitude of bulk Bloch waves at the surface.

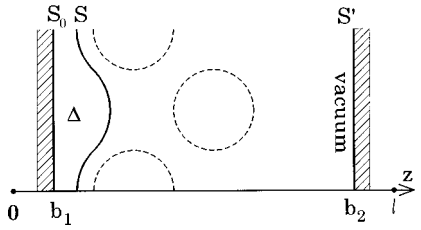

FIG. 1. Geometry for the surface-embedded Green-function calculation. The curvy embedding surface on the substrate side, S, is simulated by a plane-embedding surface S_0.

In the present work, the electronic structure of semi-infinite crystals is calculated within local-density-functional theory[5] using the embedding approach of Inglesfield.[6] The ion cores are represented by norm-conserving pseudopotentials.[7] The effects of the semi-infinite substrate and vacuum are expressed via the complex potentials acting on two embedding surfaces, S and S' ($z=b_2$) (see Fig. 1). To avoid overlapping with the ion-core region where the pseudopotential is nonlocal, the true embedding surface dividing the surface and substrate regions, S, must be curved in a complex way. However, it is too complicated to treat such a curvy surface in numerical computations. As was shown by Crampin *et al.*,[8] it is possible to define a plane-embedding surface S_0 ($z=b_1$) that simulates embedding on S.

The ground-state calculation consists of two independent steps. First, the embedding potential of the substrate on S_0 is generated for a set of $\mathbf{k}$ and energy mesh points from the bulk crystalline potential.[9] Next, the self-consistent surface Green-function calculation is performed in the embedded surface region to determine the ground-state charge density and potential energies. In doing so, the Green function at a given $\mathbf{k}$ point is expanded with a nonorthogonal plane-wave-like basis set as $G(\epsilon,\mathbf{k},\mathbf{r},\mathbf{r}')=\Sigma_{i,i'}G_{ii'}f_i(\mathbf{r})f^*_{i'}(\mathbf{r}')$, where

$$f_i(\mathbf{r})=\sqrt{\frac{2}{Sl}}\exp[i(\mathbf{k}+\mathbf{g})\cdot\mathbf{x}]\sin(p_n\ z)\quad(b_1\leqslant z\leqslant b_2) \tag{4}$$

where $p_n=\pi n/l$ ($n\geqslant1$), $\mathbf{g}$ is a 2D reciprocal-lattice vector corresponding to the 2D lattice in the xy plane, and i stands for a set of indices $(\mathbf{g},n)$. $G_{ii'}$ is calculated as $[\epsilon S-H]^{-1}_{ii'}$, where S and H are the overlap and Hamiltonian matrices, respectively. More details of the calculational method were described in Ref. 10.

After the self-consistent surface potential is obtained, we perform an additional Green-function calculation, where the normal derivative of the Green function on S_0 is forced to vanish instead of satisfying the boundary condition imposed by the embedding potential of the substrate. According to the embedding theory,[6] the surface inverse of this particular Green function on S_0, $G^{-1}_{S_0}$, provides a generalized logarithmic derivative of one-electron wave functions satisfying the outgoing (propagating or decaying toward the vacuum) boundary condition at $z=+\infty$. Thus the surface wave function ψ_ξ with a 2D wave vector $\mathbf{k}$ satisfies, on S_0,

$$\frac{\partial\psi_\xi(\mathbf{x},b_1)}{\partial z}=\frac{2m}{\hbar^2}\int_{S_0}d\mathbf{x}'\ \ G^{-1}_{S_0}[\epsilon(\xi),\mathbf{k},\mathbf{x},\mathbf{x}']\ \ \psi_\xi(\mathbf{x}',b_1), \tag{5}$$

where m is the bare electron mass. ψ_ξ is expanded on S_0 as[11]

$$\psi_\xi(\mathbf{x},b_1)=\frac{1}{\sqrt{S}}\sum_{\mathbf{g}}^{M}\left\{\frac{1}{v_z(\xi)}\phi_\xi(\mathbf{g},b_1)+\sum_{\nu}^{M} r(\xi,\nu)\phi_\nu(\mathbf{g},b_1)\right\}\exp[i(\mathbf{k}+\mathbf{g})\cdot\mathbf{x}], \quad (6)$$

where M is the number of $\mathbf{g}$ vectors used to expand the wave function in the numerical calculation. In Eq. (6), we used the suffix ν instead of ξ' for the scattered waves. ϕ_ν in this equation should include both the Bloch states and the evanescent waves decaying toward the interior of the metal. The method for calculating these Bloch and evanescent waves was described in Ref. 10. By substituting Eq. (6) into Eq. (5), one obtains an $M\times M$ system of linear equations for the M unknown constants $r(\xi,\nu)$. Among them, the coefficients corresponding to the reflected Bloch waves, $r(\xi,\xi')$, determine the surface resistivity.

III. RESULTS AND DISCUSSION

In this section, we use Hartree atomic units with $m=e=\hbar=1$. Results are presented for the (001) and (111) surfaces of fcc Al. The two outermost Al layers are embedded between the semi-infinite substrate and vacuum, and the potential energy in the embedded region is determined self-consistently. The spacing between the neighboring Al layers is taken as the bulk value. Calculated values of the resistivity may slightly change if the relaxation of surface layers is taken into consideration. The cutoff energy for the basis function (4) is 9 Ry, which leads to $\sim$20 ($\mathbf{k}+\mathbf{g}$) vectors at each $\mathbf{k}$ point. In calculating the surface resistivity (1), the SBZ integration is replaced by summation over $\sim 10^3$ equally spaced $\mathbf{k}$ mesh points. As the resistivity is not a variational quantity, it converges rather slowly with increasing $\mathbf{k}$ mesh points.

The origin of the xy plane is chosen as one of the top-layer atoms. For the (001) surface, the x and y axes are parallel to two edges of the square unit cell. For the (111) surface, the x axis points toward one of the nearest-neighbor atoms, and the y axis is contained in one of the three vertical reflection planes. Figure 2 shows contour maps of the calculated charge density $n_0(\mathbf{r})$ on the yz plane. Both surfaces have reflection symmetry with respect to this vertical cut plane. It is seen that the contours on the vacuum side of the top Al layer are corrugated rather weakly, implying that the nonzero $\mathbf{g}$ components of the surface barrier potential are small.

In order to demonstrate how the conduction electrons in the metal are scattered at the surface, it is convenient to consider Bloch states with $k_x=0$. Owing to the reflection symmetry about the yz plane, the velocity vectors of both the incident and reflected waves are then contained in the yz plane. As an example, we take $\mathbf{k}=(0,0.43)$ a.u. At this $\mathbf{k}$ point, we plotted the energy bands of fcc Al as a function of k_z. The result is shown in Fig. 3(a) for the Al(001) surface. The energy dispersion is symmetric about $k_z=0$ because the bulk crystal has reflection symmetry about the xy plane. The dispersion curves cross the Fermi energy at ξ_1 and ξ_2, where state ξ_1 with $v_z>0$ corresponds to the incident wave, while

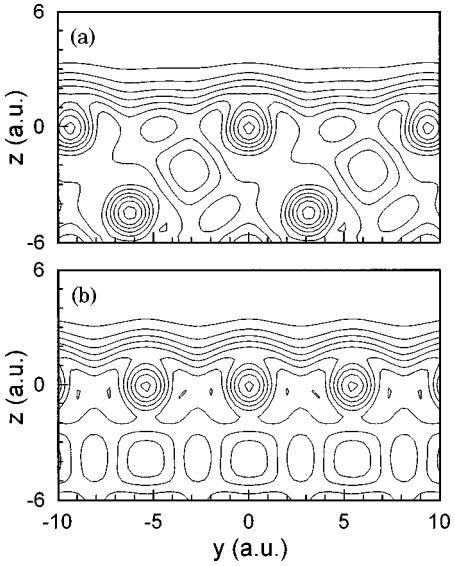

FIG. 2. Contour maps of the charge density $n_0(\mathbf{r})$ on the yz plane for (a) Al(111) and (b) Al(001). Both surfaces have reflection symmetry about this plane. The contour spacing is 0.004 a.u. The z coordinate is measured relative to the top-layer Al atoms.

state ξ_2 with $v_z<0$ corresponds to the scattered wave. Figures 3(b) and 3(c) show the energy bands of Al as a function of Δk_y, the deviation of the y component of the 3D wave vector from that of states ξ_1 and ξ_2, respectively. From the slope of the dispersion curve at $\Delta k_y=0$, one sees that they have the same negative v_y. In Fig. 3(d) we plot the

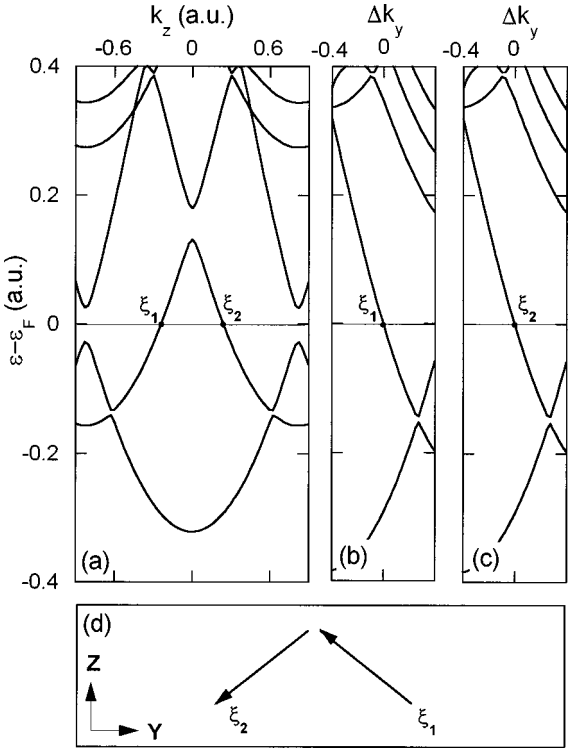

FIG. 3. (a) Energy bands of fcc Al at $\mathbf{k}=(0,0.43)$ a.u. as a function of k_z for the Al(001) surface. States ξ_1 and ξ_2 are on the Fermi surface. (b) Energy bands of fcc Al as a function of Δk_y for state ξ_1. (c) The same as (b) for state ξ_2. (d) Velocity vectors of the incident wave ξ_1 and reflected wave ξ_2 in the yz plane.

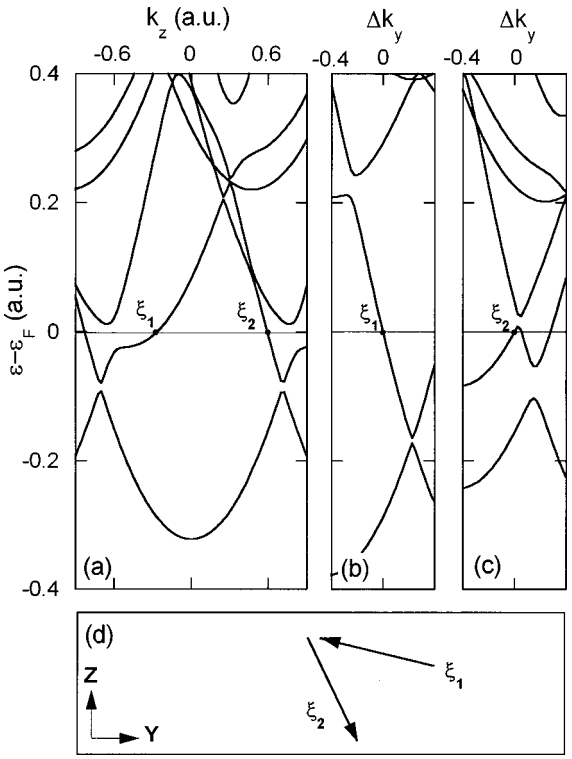

FIG. 4. (a) Energy bands of fcc Al at $\mathbf{k}=(0,0.43)$ a.u. as a function of k_z for the Al(111) surface. States ξ_1 and ξ_2 are on the Fermi surface. (b) Energy bands of fcc Al as a function of Δk_y for state ξ_1. (c) The same as (b) for state ξ_2. (d) Velocity vectors of the incident wave ξ_1 and reflected wave ξ_2 in the yz plane.

velocity vectors of the two Bloch states in the yz plane. Since there is a single pair of incident and reflected waves at this $\mathbf{k}$ point, and $\mathbf{k}$ is conserved for clean crystal surfaces, the incident wave ξ_1 is scattered to state ξ_2 with unit probability. Since ξ_2 corresponds to specular reflection, the surface wave function at this $\mathbf{k}$ point, ψ_{ξ_1}, makes no contribution to the surface resistivity.

The scenario described above is not applicable to the case of Al(111). Figure 4(a) shows the energy bands of fcc Al as a function of k_z at $\mathbf{k}=(0,0.43)$ a.u. for the Al(111) surface. Because the bulk crystal has no reflection symmetry about the xy plane, the dispersion curves are no longer symmetric about $k_z=0$. As in the case of Al(001), there is one incident wave ξ_1 with $v_z>0$ and one reflected wave ξ_2 with $v_z<0$ at ϵ_F, and, thus, state ξ_1 incident on the surface is scattered to state ξ_2 with unit probability. In Figs. 4(b) and 4(c) we show the dispersion curves of Al energy bands as a function of Δk_y for states ξ_1 and ξ_2, respectively. Because of the lower symmetry of Al(111), the dispersion curves in these two figures are not identical. It is seen that state ξ_1 has a negative v_y, whereas state ξ_2 has a positive v_y. Hence, as shown in Fig. 4(d), the Bloch electron ξ_1 changes the direction of propagation in the y direction when it is scattered at the surface. Equation (1) indicates that there is an appreciable contribution to ρ_s^{yy} at this $\mathbf{k}$ point. It should be noted that the large scattering angle of the incident wave ξ_1 does not imply that the Al(111) surface has a strong scattering potential. It only means that there is no Bloch wave in the bulk metal that can propagate in the direction of specular reflection.

For the (001) and (111) surfaces of fcc crystals, the surface resistivity is isotropic and written as $\rho_s^{\alpha\beta}=\delta_{\alpha\beta}\ \rho_s$. As for Al(001), the $\mathbf{k}$ points in $\sim$40% of the SBZ have one incident Bloch wave and one scattered wave on the Fermi surface. Because the scattered wave propagates in the specular direction for the (001) geometry, this area of the SBZ makes a vanishing contribution to the resistivity ρ_s. As discussed above, this is not the case for the (111) surface. As for Al(111), the $\mathbf{k}$ points in $\sim$60% of the SBZ have a single pair of incident and scattered Bloch waves at ϵ_F. According to our calculation, this region of the SBZ still contributes up to 52% of the total resistivity. Thus the second mechanism, as discussed in Sec. I, is very important for the surface resistivity of clean metal surfaces. We note that the contribution to ρ_s from this $\mathbf{k}$ region does not depend on the structural relaxation of surface layers as far as the original surface unit cell remains intact. This is because Δv_α in Eq. (1) is a bulk property, and the scattering probability $p(\epsilon_F,\xi,\xi')$, which depends in principle on the surface scattering potential, is equal to unity in this $\mathbf{k}$ region.

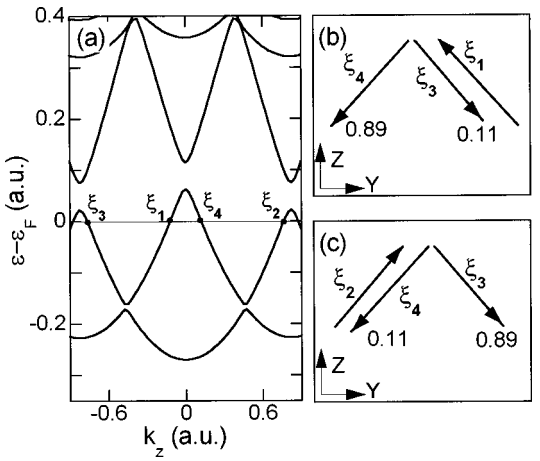

FIG. 5. (a) Energy bands of fcc Al at $\mathbf{k}=(0,0.54)$ a.u. as a function of k_z for the Al(001) surface. (b) Velocity vectors of the incident and reflected waves for the surface wave function ψ_{ξ_1}. (c) The same as (b) for ψ_{ξ_2}. The small numbers near each scattered wave indicate the scattering probability $p(\epsilon_F,\xi_i,\xi_j)$ ($i=1$ and 2 and $j=3$ and 4).

For the (001) surface, the surface resistivity arises from the Umklapp process. The $\mathbf{k}$ points with two pairs of incident and scattered Bloch waves at ϵ_F occupy $\sim$50% of the SBZ, and those with more than two pairs occupy $\sim$10% of the SBZ of Al(001). As an example, let us consider $\mathbf{k}=(0,0.54)$ a.u. In Fig. 5(a), we show the energy bands of fcc Al as a function of k_z at this $\mathbf{k}$ point for the Al(001) surface. There are four Bloch states on the Fermi surface. Among them, states ξ_1 and ξ_2 with $v_z>0$ correspond to incident waves, and states ξ_3 and ξ_4 with $v_z<0$ are reflected waves. In Figs. 5(b) and 5(c), we show the velocity vectors and scattering probability of the two surface wave functions ψ_{ξ_1} and ψ_{ξ_2}. The calculated velocities are $(v_y,v_z)=(-0.607,0.656)$ a.u. for state ξ_1 and $(v_y,v_z)=(0.535,0.621)$ a.u. for state ξ_2. The incident wave ξ_1 contributes to the surface resistivity when it is scattered to the off-specular beam ξ_3. The calculated probability for this event, $p(\epsilon_F,\xi_1,\xi_3)$, is, however, only 0.11. With a much

larger probability, state ξ_1 is scattered to state ξ_4, corresponding to specular reflection. The same is true for the incident wave ξ_2. It should be noted that the relationship $p(\epsilon_F,\xi_1,\xi_3)=p(\epsilon_F,\xi_3^*,\xi_1^*)=p(\epsilon_F,\xi_2,\xi_4)$ holds. The first equality is the reciprocity relation, whereas the second holds because the two $\mathbf{k}$ points $(0,k_y)$ and $(0,-k_y)$ are symmetrically equivalent for the (001) surface.

In the case of clean metal surfaces, the surface resistivity ρ_s scales in inverse ratio to the film thickness l_f because the surface occupies $1/l_f$ of the total volume of the crystal. The calculated resistivity is $l_f\rho_s=0.59$ a.u for Al(001) and $l_f\rho_s=3.54$ a.u. for Al(111). In evaluating these values, we have used $m^*/m=1.42$ as the effective mass $m^*_{\alpha\beta}=\delta_{\alpha\beta}\ m^*$ in Eq. (1). This value is calculated from

$$\frac{1}{m^*}=\left\langle\frac{1}{m^*}\right\rangle_{zz}=\frac{1}{\pi\hbar n_e}\int_{\mathrm{SBZ}}\frac{d\mathbf{k}}{(2\pi)^2}\sum_{k_z,n}|v_z(\xi)|, \qquad (7)$$

where the summation is taken over all the incident and scattered waves on the Fermi surface.[12] The measured resistivity of bulk Al at a room temperature ($T=273$ K) is $\rho_b=2.5\ \mu\Omega$ cm$=0.11$ a.u.[13] Assuming $l_f=10^3$ Å, we find that the surface contributes to 1.7% of the total resistivity of the film for the Al(111) surface. This ratio increases with decreasing temperature and reaches $\sim 10\%$ at $T\sim 100$ K. Therefore, the resistivity induced by defect-free crystal surfaces is not negligible at all in treating thin metallic films.

As stated above, the resistivity of the Al(111) surface is ~ 6 times larger than that of the Al(001) surface. This indicates that the second mechanism for the resistivity of clean metal surfaces as described in the present paper is quite important. Since this mechanism is not related with any specific properties of the Al band structure, we expect that a similar trend in the crystal-face dependence of the resistivity may generally be observed in many fcc and bcc metals, i.e., the resistivity of the (111) surface would be considerably larger than those of the (001) and (110) surfaces.

IV. SUMMARY

We have studied the resistivity of ideal crystal surfaces of semi-infinite metals. For clean surfaces, the crystal momentum in the surface plane is conserved when conduction electrons in the metal are scattered at the surface. Nevertheless, their velocity in the plane can be changed due to two mechanisms: The first is the Umklapp process, and the second arises when the bulk crystal has no reflection symmetry about the crystal plane corresponding to the surface. Both contribute to the resistance of the system. We have performed a density-functional calculation and evaluated the resitivity of low-index surfaces of Al. It was found that the resistivity of the smooth and close-packed Al(111) surface is much larger than that of the more loosely packed Al(001) surface, owing to the second mechanism. It is expected that this counterintuitive result may hold for other fcc metals.

ACKNOWLEDGMENT

This work was supported by a Grant-in-Aid from the Ministry of Education, Science, and Culture of Japan.

[1] D. Schumacher, *Surface Scattering Experiments with Conduction Electrons*, Springer Tracts in Modern Physics Vol. 128 (Springer, Berlin, 1993).

[2] *Physics of Sliding Friction*, edited by B. N. J. Persson and E. Tosatti (Kluwer, Dordrecht, 1996).

[3] A. Liebsch, *Electronic Excitations at Metal Surfaces* (Plenum, New York, 1997).

[4] H. Ishida, Phys. Rev. B **52**, 10 819 (1995).

[5] W. Kohn and L. J. Sham, Phys. Rev. **140**, A1133 (1965).

[6] J. E. Inglesfield, J. Phys. C **14**, 3795 (1981).

[7] The ion-core pseudopotential is generated using a method of N. Troullier and J. L. Martin [Phys. Rev. B **43**, 1993 (1991)] and casted in the Kleinman-Bylander form [Phys. Rev. Lett. **48**, 1425 (1982)].

[8] S. Crampin, J. B. A. N. van Hoof, M. Nekovee, and J. E. Inglesfield, J. Phys.: Condens. Matter **4**, 1475 (1992).

[9] The bulk electronic structure is calculated using a plane-wave computer code based on the standard conjugate-gradient method [M. P. Teter, M. C. Payne, and D. C. Allan, Phys. Rev. B **40**, 12 255 (1989)].

[10] H. Ishida, Surf. Sci. **388**, 71 (1997).

[11] The wave function ψ_ξ on S_0 has no physical meaning. Given a ψ_ξ and its normal derivative on S, ψ_ξ on S_0 is obtained by integrating the Schrödinger equation from S through the volume Δ to S_0. The Bloch and evanescent waves on S_0 in Eq. (6) are defined in the same way. See Ref. 10 for more details.

[12] We calculated $(1/m^*)_{zz}$ instead of $(1/m^*)_{xx}$. They are identical for fcc crystals. $(1/m^*)_{xx}$ can be calculated by replacing $|v_z(\xi)|$ in Eq. (7) by $v_x(\xi)^2/|v_z(\xi)|$. However, it was found that this integral is less stable because of the denominator $|v_z(\xi)|$.

[13] The bulk resistivity of Al at 295 K given in Ref. 4, $\rho_b=1.3$ a.u., should be corrected as $\rho_b=0.13$ a.u.